INVESTIGATION ON MOISTURE MONITORING IN MASONRY STONES USING A WIRELESS LC RESONANT SENSOR

J. H. Zhao
University of Manitoba, Canada

D. J. Thomson
University of Manitoba, Canada

M. Uddin
University of Manitoba, Canada

A. A. Mufti
University of Manitoba, Canada

The presence of moisture in the masonry structures has a great impact on the strength and integrity of building. Moisture controlling paradigms for preventing structural deterioration and performance degradation from the water content require effective moisture monitoring systems. However, most moisture sensors require the use of wires. This paper presents a wireless, passive inductor-capacitor (LC) resonant circuit technique for measuring the moisture level within application to heritage masonry building stones. The sensor monitors capacitance changes between embedded electrodes, induced by the variation of the effective dielectric constant due to the presence of water in the stone. The corresponding change of the resonant frequency can therefore be used to monitor the water content of the stone. The operation of the sensor was demonstrated with dry sandstone samples placed in a water bath, allowing moisture to be transported into the sandstone surrounding the electrodes of the capacitor. The rise in capacitance resulted in a resonant frequency decrease from 5.96 MHz to 5.21 MHz while the moisture RH sensor indicated the relative humidity inside the stone changed from about 10% to 100%. The moisture variations were investigated for both the wetting and drying cycling processes. The RH sensor was found to be saturated at 100% over a wide range of stone moisture conditions. Since the electrical signal can be inductively transmitted between two spiral inductors in separate positions, wireless monitoring of the civil structural health becomes possible without requiring batteries.

Corresponding author's email: thomson@ee.umanitoba.ca

INVESTIGATION ON MOISTURE MONITORING IN MASONRY STONES USING A WIRELESS LC RESONANT SENSOR

J. H. Zhao, D. J. Thomson, M. Uddin and A. A. Mufti
University of Manitoba, Winnipeg, Canada

ABSTRACT: The presence of moisture in the masonry structures has a great impact on the strength and integrity of building. Moisture controlling paradigms for preventing structural deterioration and performance degradation from the water content require effective moisture monitoring systems. However, most moisture sensors require the use of wires. This paper presents a wireless, passive inductor-capacitor (LC) resonant circuit technique for measuring the moisture level within application to heritage masonry building stones. The sensor monitors capacitance changes between embedded electrodes, induced by the variation of the effective dielectric constant due to the presence of water in the stone. The corresponding change of the resonant frequency can therefore be used to monitor the water content of the stone. The operation of the sensor was demonstrated with dry sandstone samples placed in a water bath, allowing moisture to be transported into the sandstone surrounding the electrodes of the capacitor. The rise in capacitance resulted in a resonant frequency decrease from 5.96 MHz to 5.21 MHz while the moisture RH sensor indicated the relative humidity inside the stone changed from about 10% to 100%. The moisture variations were investigated for both the wetting and drying cycling processes. The RH sensor was found to be saturated at 100% over a wide range of stone moisture conditions. Since the electrical signal can be inductively transmitted between two spiral inductors in separate positions, wireless monitoring of the civil structural health becomes possible without requiring batteries.

1 INTRODUCTION

The transport and storage of moisture in building envelop structures are important issues in civil engineering and building physics, considerable engineering practices and theoretical simulations (such as heat, air and moisture modelling (HAM)) have been exercised to mitigate moisture induced structural deterioration, performance degradation and growth of moulds in the building enclosure components (Straube 2002/2001 & Tariku 2009). The efficient moisture controlling methodologies significantly rely on effective moisture monitoring systems so as to ensure proper maintenance of durability and functionality of the building structures and materials (Glass 2007 & Maurenbrecher 2000). Currently, Most commercially available moisture monitoring meters and instruments are mainly based on the electrical properties that changes with moisture content inside the building structures and materials. As water is more electrically conductive and its dielectric permittivity is much higher than that of construction materials, the dependence of the electrical conductivity and the dielectric permittivity on the water content forms resistance-, capacitance- and microwave-based methods (Said 2004). Since the moisture problems exhibit diverse and complex natures due to a wide variety of materials/structures and complicated in-situ physical/electromechanical processes as well as largely variable harsh climate conditions, the existing moisture measuring technologies usually have the limited functionalities and adeptability in fully meeting the field monitoring requirements (Said 2004 & Onysko 2008). For examples, the resistance method monitors the wetness level by measuring the conductance of materials, the challenges facing by it come from instrumentations dealing with a wide range of electrical resistance varing from a few ohms to several hundred MΩ, also, salt ions movements and accumulation around the electrodes, which, in the presence of an electric field, often causes the polarization of the material under testing. The dielectric based methods are strongly influenced by surface moisture content with its normal calibration (Roveti 2001). Therefore, considerable scientific and engineering efforts have been continually devoted to developing more effective sensing technologies. In paticular, recent rapid development of wireless sensing technology to the application in health structure monitoring have received both academic and industrial interests (Lynch 2006) because wireless monitoring systems are less expensive to install as wiring between sensors and data acquisition systems required for tethered monitoring systems is not required. Since power consumption is a major issue for the wireless sensors operating on batteries, considerable engineering efforts have been made to develop battery-free wireless sensors, such as radio-frequency identification sensors (RFID) and wireless passive inductive telemetric sensors for moisture monitoring (Sidén 2007, DeHennis 2005 & Marioli 2011).

Considering that most of the heritage structures in Canada use three conventional Canadian masonry stones, (e.g. St. Canut and Ohio sandstone, and limestone) and the cultural heritage buildings require preserving their original exterior appearance and texture by preservation guidelines (Uddin 2009), it is necessary to choose the monitoring systems able to be embedded inside the structures without external wiring. With this in mind we have applied a simple and cost effective technique for monitoring moisture level inside the masonry stones using an inductive telemetric measurement system which basically consists of an inductance-capacitance (LC) resonant circuit. The LC sesoant sensor takes very simply configured capacitive and inductive component to measure the moisture content inside the stone, the experimental results demonstrate the sensor's promising potential in the field application of the moisture monitoring.

2 APPARATUS AND EXPERIMENT

The LC resonant circuit moisture sensor is composed of an inductive sensing coil and a capacitor formed by two stainless steel rods, as schematically shown in Figure 1(a), where the sensing inductive coil was made by winding 20 turns of wires on a PVC tube of 8.4 cm diameter, the capacitor was composed of the two parallel steel bars with a diameter of 5 mm and length of 7 cm, and located inside the two holes drilled in the sandstone. Another inductive interrogator coil, a 5-turns coil of 5.1 cm diameter wound by an insulated wire of 1.2 mm diameter, was built as a signal transmitter and receiver. When the interrogator coil is positioned near the sensing coil, the electrical signal can be inductively transferred back and forth between the two coils. The signal, carrying with the resonant characteristic of the sensing LC circuit, was captured using the Agilent Impedance Analyzer through the interrogator coil, and the impedance of the whole electrical system, composed of the interrogator coil and the sensing coil, was hence measured. The equivalent electrical circuit of the experimental setup is schematically captured as shown in Figure 2, which was used to simulate the electrical behaviour using the SPICE model [PSpice^{TM} student version]. For the sensing coil, its series inductance is of L_S = 63.67 µH, its series resistance takes R_S = 17 Ω, and its parasitic capacitance is of C_p = 4.6 pF. The coil has a self-resonant frequency of 9.37MHz. The two-bars capacitor in the stone gives a capacitance of C_p= 5.32 pF and conductance of G = 3.9 µS measured at the frequency of 6 MHz using the Impedance Analyzer. The whole sensing LC system gives the measured resonant frequency of 5.96 MHz in the lab environment. The interrogator coil has a series inductance of Ls = 2.35 µH, a series resistance of Rs = 0.334 Ω and a self-resonant frequency of fres = 28.32 MHz (Bhadra 2010).

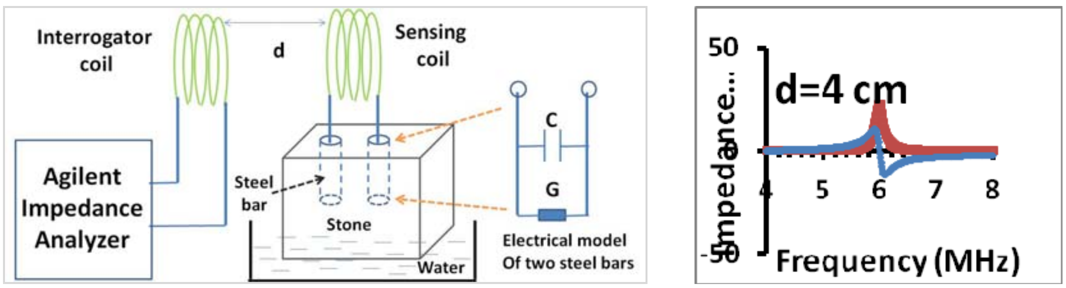

(a) (b)

Figure 1. (a) Experimental setup for testing inductive coil sensors using impedance measurement technique. (b) The impedance resistance peaks at the resonant frequency of the sening LC circuit.

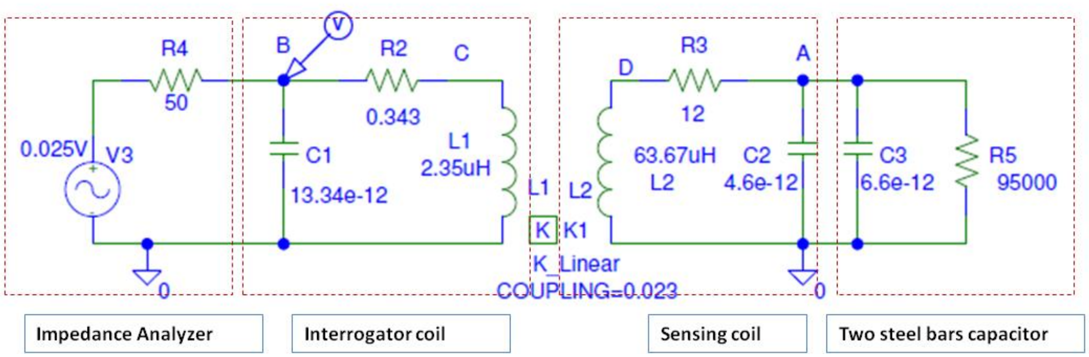

Figure 2. The equivalent electrical circuit of the LC resonant sensing system

The resonant frequency of the LC sensing element, composed of the inductive sensing coil in parallel with the two-bars capacitor, can be calculated based on the equivalent LCR electrical circuit as shown in Figure 2:

$$f_r = \frac{1}{2\pi}\sqrt{\frac{1}{L_2(C_2+C_3)}} \quad [1]$$

$$Q = \left(\frac{R_2}{\omega L_2} + \frac{\omega L_2}{R_5}\right)^{-1} \quad [2]$$

Where the resonate frequency f_r is defined as the frequency at the maximum of the real part of the impedance resistance, which depends on the inductance L_2 of the sensing coil, the parasitic capacitance C_2 of the coil and the capacitance C_3 of the two-bars capacitor. Quality factor Q reflects the energy loss of the sensing system which is largely affected by the series resistance of R_2 and the effective resistance R_5 related to the dielectric loss of the two-bars capacitor.

A typical frequency dependent impedance of the sensing LC circuit was measured by the Impedance Analyzer through the interrogator coil as shown in Figure 1(b), where the distance between the sensing coil and interrogator coil is 4 cm, the signal was extracted out by subtracting the background contributed by the interrogator coil. The maximum of the real part (R) and the zero reactance (X) occurs at the almost same resonant frequency of 5.96 MHz because the dielectric loss is very small when the whole testing system sitting in the lab prior to the wetting.

As shown in Figure 1(a), the two parallel bars behave electrically as a capacitor in parallel with a conductor, its capacitance and conductance are dependent on both physical dimension and the surrounding dielectric medium. The electrical circuit model can be understood by considering the dielectric medium exhibiting complex relative dielectric permittivity at the radio and microwave frequency as the following:

$$\varepsilon_r(\omega) = \varepsilon_r'(\omega) - j\varepsilon_r''(\omega)$$
(3)

The real part ε_r' is related to the capacitive response of a material and often called as the ‘dielectric constant’, the imaginary part ε_r'' is related to the conductive response and referred to as the ‘dielectric loss’. The equivalent electric circuit for the two bars can be characterized mathematically using the following formula:

$$Y = j\omega C_0(\varepsilon_r' - j\varepsilon_r'') = G + jB$$
(4)
$$B = \omega C_0 \varepsilon_r'$$
(5)
$$G = \omega C_0 \varepsilon_r''$$
(6)

Where the admittance Y is defined as the inverse of the impedance, measuring how easily a circuit or a device will allow a current to flow. G is the conductance (Siemens) as related to the $\varepsilon_r''(\omega)$, and B is the susceptance (Siemens) as related to the $\varepsilon_r'(\omega)$, which, here in our experiment, will be greatly affected with the water content inside the materials. For pure water, $\varepsilon_r'(\omega) \approx 80$ under the low-frequency (<50MHz) (Pringle 2008). In contrast to the other civil materials, $\varepsilon_r'(\omega)$ is highly sensitive to the fraction of liquid water at microwave frequencies, e.g., $\varepsilon_r' = \varepsilon_r'(stone) + D_w \cdot \varepsilon_r'(water)$, where D_w is the volumetric perentage of water moisture with regard to the stone. In addition, since the effective loss factor $\varepsilon_r''(\omega)_{eff} = \varepsilon_r'' + \sigma / \varepsilon_0 \omega$, for the materials with the presence of the dissolved salts, $\varepsilon_r''(\omega)_{eff}$ increases via enhanced ionic conduction.

When the two-bars capacitor starts sensing the moisture entering its electrical field region, the capacitance increases significantly due to the increase of the dielectric constant of the surrounding medium resulted from the high dielectric constant of water. This results in the decrease in the sensor's resonant frequency based on the formula (1). In addition, the electrically more conductive water also increases the dielectric loss of the capacitor, leading to the reduction in the amplitude of the resistance. In our testing setup, only the capacitance of the two-bars changes with the water level inside the stone while the inductance of the sensing coil keeps constant, the variation of the resonant frequency of the sensor directly reflects the water level. In the following section, the data for the impedance variation during the wetting and drying process will be discussed and the corresponding water transport properties inside the stone will be analyzed.

3 RESULTS AND ANALYSIS

The masonry stones under testing were contributed by the Public Works of Canada. Previously, the same types of stones were tested on the compatibility between anchoring materials and the masonry stones through slow freeze-thaw cycles in both dry and saturated conditions carried out in the ISIS Canada (Uddin 2009).

The moisture content in the sandstone was tested using the LC sensor when the stone was put in a water container. The testing was carried out in the laboratory environment. The de-ionized water and the stone were sitting in the lab and the room temperature was supposed to be constant during the course of the measuring. The relative humidity in the lab is around ((10±2)%) and the ambient temperature is around (22±1)°C, which were measured using a thermo-anemometer (Alnor Compuflow Model 8585). In order to evaluate the moisture in the stone, the relative humidity (RH) sensor (Honeywell HCH-1000) was employed to measure the RH inside the stone so that the RH variation and the resonant frequency shift of the LC sensor in the stone can be compared corresponding to the moisture level in the stone. The RH sensor was inserted into a hole drilled into the stone near the two-bars capacitor in the same horizontal position so that both the two-bars and the RH sensor would simultaneously sense the coming moisture. The RH inside the stone was obtained by measuring the capacitance of the RH sensor using the Impedance Analyzer, the capacitance values were then converted into the RH based on the calibration data from the datasheet of the RH sensor, the RH has a linear relationship with the capacitance in the range of 0-100% RH, the sensitivity is of 0.55 pF/%RH to 0.65 pF/%RH (data sheet of Honeywell HCH-1000). In addition to the measuring of the RH, the stone weight increase, relative to the moisture-free drying state, was also measured to evaluate the moisture content inside the stone corresponding to each measurement of the RH and the resonant frequency.

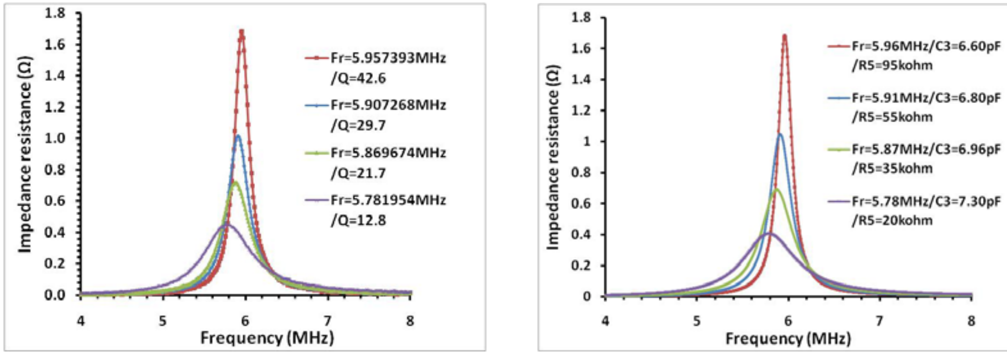

(a) (b)

Figure 3. (a) The experimental data show the resonant frequency and the peak amplitude increase during the drying. (b) The simulation results show the exact electrical resonant behaviour as the measured.

According to the equivalent electrical circuit in Figure 2, the resonance of the sensing circuit were transferred to the interrogating circuit through the mutual induction between the sensing coil and the interrogator coil, then the resonant behaviour was captured through measuring the impedance. Figure 3(a) shows the frequency dependent impedance measured during the drying process, it can be seen that the resonant frequency at the peak resistance increased with the continuing drying since the capacitance of the two bars (C_3) decreased, the peak amplitude increased and the peak width became narrower because the dielectric loss induced by the moisture reduced. This impedance behaviour was simulated using PSPICE simulator by choosing the capacitance of the C_3 and resistance R_5 based on the resonant frequency and the loss factor (Q) from the measured experimental data, as shown in the Figure 3b. The simulation data agrees very well with the experimental data, showing that the decrease in the resonant frequency corresponds to the increase in the capacitance and the amplitude of the resonant impedance decreases with the reduced resistance between the two electrodes.

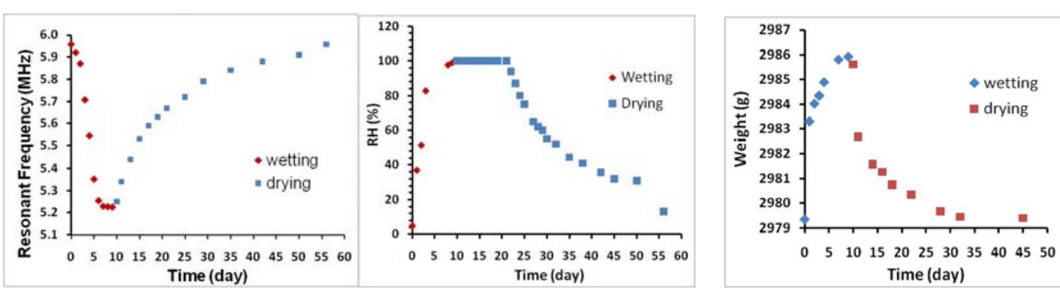

(a) (b) (c)

Figure 4. (a) Resonant frequency versus time, (b) RH values versus time, (c) Weight of stone versus time

The testing for the wetting and drying cycling was carried out. The resonant frequency, corresponding to the moisture level, which is represented with the wetting and drying time, was measured as shown in Figure 4(a). It can be clearly seen that the resonant frequency decreased during the wetting and increased during the drying. Simultaneously, the RH values inside the stone during the wetting and drying were measured as shown in the Figure 4(b). The RH relatively quickly changed to around 85% in first 4 days and subsequently reached 100% in the following 4 days. After that, the stone was taken out the water container and sitting in the lab for naturally drying. The RH sensor kept constant value (100%) in about 10 days, then started gradually decreasing, finally back to the state as that before the stone was put into the water in almost a month. both the data for the RH and resonant frequency, on the one hand, strongly support the resonant frequency shift is capable of correctly tracking the moisture level; on the other hand, suggest that the RH sensor fail fully reflecting the water content once the sensor were saturated due to the excess water while the LC sensor is able to continuously monitor the water level through detecting the resonant frequency change. Additional conclusions suggested from the data are that water absorption into the stone during the wetting is much faster than water's desorption during the drying. This means the trapped water inside the stone takes much longer time to exit once water transported into the masonry stone walls due to water absorption, for example, due to rain.

The measurement of the RH inside cavities in the stone is very difficult to covert to water content. In practice, accurate evaluation of the water content is carried out by weighing the materials in the dry state and in the wet state, respectively. All other measuring methods have to be correlated the real water content and calibrated with the real water content for the specific materials. The relationship between the percentages of the water weight relative to the weight of the dried materials should be established for the moisture measuring systems. In our experiment, the weight of the stone during the wetting and drying was measured along with the each measurement of the impedance and the RH, as shown in Figure 4(c). The weight increased for about 4 gram in the first wetting day, then, additional 2.5 gram water moisture went into the stone in the subsequent 7 days. This means the water transport into the stone at the very beginning was fast and then slowed down, indicating the mechanisms for water transporting in the stone are different for the beginning stage of the wetting and the subsequent transport stage. The portion near the stone surface in contact with the water first absorbed most of the water, most likely through capillary effect. The water moisture transports inside the stone mainly in the forms of both vapour diffusion and capillary effect. The transport properties depend on the specific physical (mineralogical) structure and the density of the stone (Beck 2003 & Künzel 2009). Based on the measured weight variation in a range of a few grams, it suggests that the sandstone under testing is relatively dense. Nevertheless, with such a small amount of the water the relative humidity can reach 100% RH easily. In addition, the moisture condensation could occur when the RH of 100% was reached due to temperature variation, causing failure in correctly detecting the moisture level using the RH sensor. This is suggested by the measured data for which the RH maintained constantly for a long period of time during the drying process.

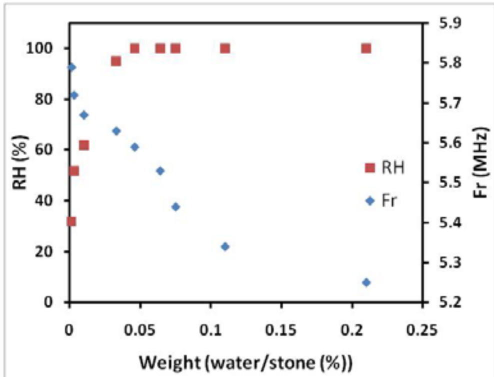

(a)

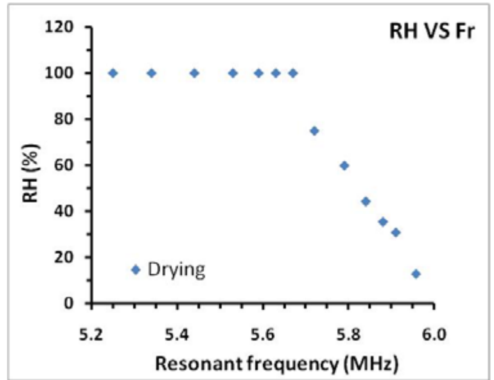

(b)

Figure 5. (a) The resonant frequency shift and the RH versus the water weight percentage relative to the drying stone. (b) The correlation between the measured resonant frequency and the RH.

Figure 5(a) shows the RH and the resonant frequency variation corresponding to the weight change of the stone during the course of the drying. As clearly seen, once the RH sensor was saturated it did not change despite the weight of the wetted stone reduced a lot during the drying. Only when the water content dropped below 0.05%, the RH sensor started to work and the RH value decreased with the continuing drying. In contrast, the resonant frequency shows the monotonic increase during the drying, though not linearly with the water/stone weight percentage. Figure 5(b) plotted the correlation between the RH and the resonant frequency of the LC sensor for our stone testing system. It can be seen that there is a rough linear relationship between the RH and the resonant frequency corresponding to the resonant frequency changes from 5.2 MHz to 5.96 MHz, suggesting that the LC sensor can replace the RH senor for measuring the moisture up to 100%RH. The data positively demonstrate that the LC sensor have more extended capability for correctly monitoring the water content comparing to the RH sensor once the correlation between the water content and the resonant frequency is established. When designing the measurement instrument, another important consideration which should be taken is the quality factor of the resonant system. How far the detecting ability of the LC moisture sensor can be extended depends on how high the quality factor can be maintained to meet the instrumentation requirements pertaining to the dielectric loss and the ionic conduction in the materials due to the existence of water.

4 CONCLUSION

This paper has presented the moisture testing inside the masonry stones using a wireless, passive LC resonant sensor. This simple and cost-effective sensor is based on an inductor-capacitor resonant circuit. The sensor was able to detect varying amounts of water in the masonry sandstones by measuring the change in the sensor's resonant frequency. The sensor performance during the wetting and drying cycling process was investigated, showing the resonant frequency decrease in the wetting and increases in the drying. In contrast with the RH sensor, the LC sensor is capable of measuring the moisture content well beyond the range where RH sensor mounted in cavities in the stone becomes saturated. The data of the sensor's resonant frequency obtained from the tests can be correlated to the water-to-mass ratio of the samples, demonstrating the viability of the LC moisture sensor technology for use in civil infrastructures.

ACKNOWLEDGMENTS

This work is supported by Public Works Canada and the ISIS (Intelligent Sensing for Innovative Structures) Canada Resource Centre, The Canadian Microelectronics Corporation, The Canada Foundation for Innovation and the Province of Manitoba. The assistance with the sample preparation from Chad Klowak is gratefully acknowledged.

REFERENCES

Beck, K, Al-Mukhtar, M, Rozenbaum, O & Rautureau, M. (2003). Building and environment, 38, pp.1151.

DeHennis, AD & Wise, KD. (2005). Journal of Microelectromechanical Systems, 14, pp. 12.

Glass, SV. (2007). ASHRAE.

Lynch, JP & Loh, KJ. (2006). The Shock and Vibration Digest, pp. 92.

Künzel, HM & Holm, AH. (2009). PATORREB.

Maurenbrecher, AHP, Saïd, MNA, Ibrahim, K & Cornick, SM. (2000). Monitoring the performance of masonry building envelopes, Proceedings of the 12th International Brick/Block Masonry Conference, Madrid, Spain, 2, pp. 1221-1233.

Marioli, D, Sardini, E & Serpelloni, M. (2011). Inductive Telemetric Measurement Systems for Remote Sensing. Advances in Measurement Systems.

Onysko, DM, Schumacher, C, Garrahan, P. (2008). Journal of Building Enclosure Design.

Pringle, D, Dubuis, G, Eicken, H. (2008). J. Glaciol. 5.

Pel, L, Kopinga, K & Brocken, H. (1996). HERON, 41, pp. 95-105.

Roveti, DK (2001). Choosing a Humidity Sensor: A Review of Three Technologies, Humidity/Moisture.

Sidén, J, Zeng, X, Unander, T, Koptyug, A & Nilsson, H-E. (2007). IEEE Sensors Conference, pp. 308.

Bhadra S. (2010). Thesis, University of Manitoba.

Straube, JF and Burnett, EFP. (2001). Chapter5: Overview of Hygrothermal Analysis Methods, ASTM Manual 40- Moisture Analysis and Condensation Control in Building Envelops, American Society of testing and Materials, Philadelphia.

Straube, JF. (2002). Moisture in Buildings. ASHRAE Journal, pp.1-5.

Said, MN. (2004). Research Report #190, NRC, Institute for Research in Construction.

Tariku, F, et al. (2009). NRCC-51275.

Uddin, M, Mufti, A, Polyzois, D, Shrive, N, Jaeger, L, Stephenson, D, Duchesne, D & Paquette, J. (2009). 4th International Conference on Structural Health Monitoring on Intelligent Infrastructure (SHMII-4), Switzerland.